

**The Henryk Niewodniczański
INSTITUTE OF NUCLEAR PHYSICS
Polish Academy of Sciences
ul. Radzikowskiego 152, 31-342 Kraków, Poland**

www.ifj.edu.pl/publ/reports/2014/

Kraków, February 2014

Report No. 2071/PH

The optical alignment system for luminosity detector at ILC

Elżbieta Banaś, Witold Daniluk, Eryk Kielar, Jerzy Kotuła, Beata Krupa,
Arkadiusz Moszczyński, Krzysztof Oliwa, Bogdan Pawlik,
Wojciech Wierba, Leszek Zawiejski

Streszczenie

Możliwość użycia półprzezroczystych detektorów krzemowych do pomiaru przemieszczeń detektora świetlności LumiCal, planowanego dla przyszłego liniowego akceleratora ILC/CLIC, była badana przy pomocy optycznego systemu laserowego bazującego na tych detektorach. Wstępne wyniki pomiarów wykonanych przy użyciu prototypu tego systemu dostarczyły wartości pomiaru przemieszczeń w kierunkach X i Y z dokładnością na poziomie kilku mikrometrów.

Abstract

The possibility to use semi-transparent silicon detectors to measure the displacement detector luminosity LumiCal, planned for the future linear accelerator ILC / CLIC, was studied using an optical laser system based on these detectors. Preliminary results of measurements were achieved using the prototype of this system provided in the displacement measurement values of the X and Y directions with an accuracy of a few microns.

1 Introduction

The future e^+e^- linear collider which is a proposal from the high-energy community should be a very precise machine, not only able to verify the results obtained at the LHC but also serve as a unique device in the search for signals of new physics. This idea is now developed under the ILC [1] (International Linear Collider) and CLIC [2] (Compact Linear Collider) projects and the LCC (Linear Collider Collaboration) [3] was established to better coordinate the work carried out around the world for the needs of both these projects. Two main detectors are planned for physics studies working in a pull-push mode and for ILC project – they are called ILD (International Large Detector) [4] and SiD (Silicon Detector) [5]. In the framework of ILD, the luminosity detector LumiCal will be located in a very forward region together with BeamCal and BeamCal Pair Monitor, the two other detectors studied by FCAL collaboration [6,7]. The FCAL detectors are designed to cover the area of small polar angles in the range of 5 - 80 mrad. Figure 1 illustrates this situation.

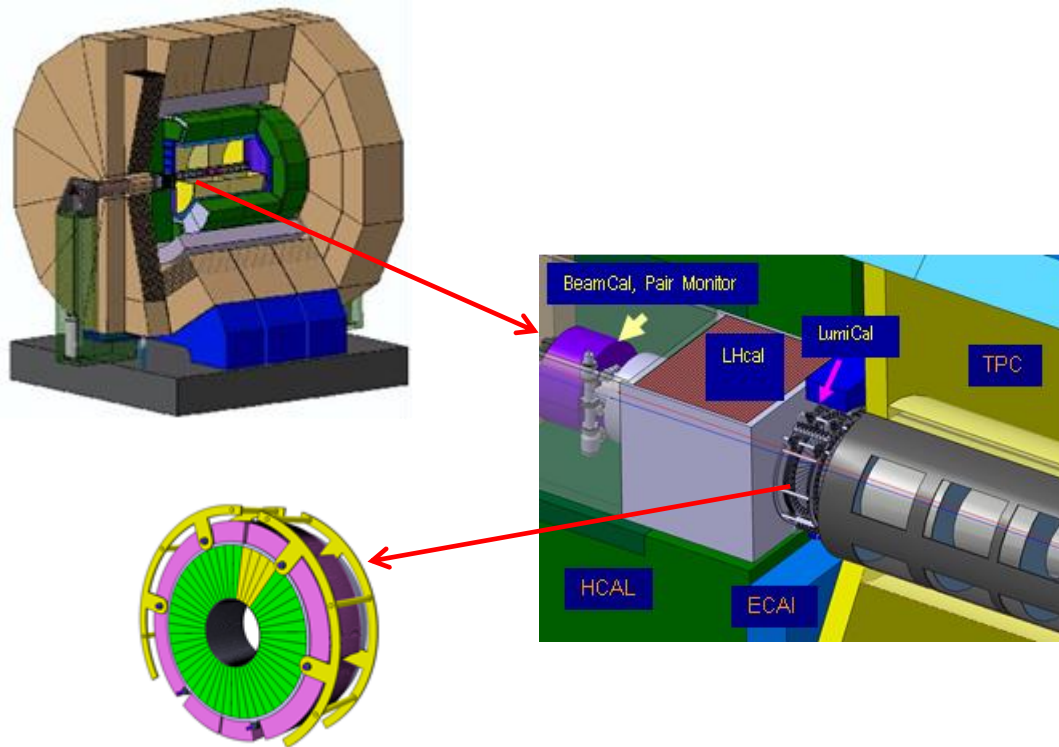


Figure 1. Location of detectors of the FCAL collaboration inside the main detector ILD. The yellow sectors of the silicon sensors visible for LumiCal are used in beam tests at the DESY test beam facility.

The LumiCal detector, which contains two silicon-tungsten calorimeters, is expected to provide the required precision of the luminosity measurement and to extend calorimetric coverage mainly for electrons and photons at polar angles between 30 and 80 mrad. The luminosity measurement will be based on the determination of the Bhabha events rate and the relative precision of the integrated luminosity ($\Delta L/L$) better than 10^{-3} will be achievable. To

fulfil this task it is necessary to build a detector with micrometer precision and to have an online laser positioning system for a displacement monitoring of LumiCal with an accuracy of a few hundred micrometers as well as the displacement of its internal layers with an accuracy of a few micrometers. The integration of the LumiCal with the ILD raises a number of questions on the topic of MDI (Machine Detector Interface) related to available free space for the laser alignment system (LAS), choice of QD0 magnets [4] as possible reference systems and the detector installation procedure. Another problem can stem from general requirements to have easy access to the subdetectors. Hence, further extensions and modifications of the LAS are necessary. It is necessary to control the displacement of the LumiCal detector during physics running to receive the required accuracy in luminosity measurements. For this purpose the alignment system is designed for LumiCal which will provide the knowledge about absolute distances between both LumiCal (Left and Right) calorimeters as well as the relative position of each of them to the corresponding reference frame like QD0 magnets. The acceptable values are on the level of 100 microns in Z direction over the distance of 5 m, and about 500 microns for transversal (X,Y) displacements. In addition, the inner radius of the silicon sensors layers has to be known with an accuracy better than 4 microns as well as the positions of the internal sensors layers in calorimeters with an accuracy of a few microns. The work on alignment of the LumiCal is performed partly within AIDA [8] project as a continuation and extension of studies done previously in the EUDET [9] project. The goal is to prepare the laboratory prototype of laser alignment system (LAS) and then to test it together with the calorimeter module, built in the AIDA project, on beam tests measurements. Output data from the alignment system will be integrated with DAQ of the AIDA LumiCal calorimeter module.

2 Laser alignment system

One of the possible solutions proposed for monitoring the movements of the LumiCal detector is the LAS system containing two components: one with semi-transparent silicon sensors and the second with interferometric method of the distance measurement based on the FSI (Frequency Scanned Interferometry) approach [10]. Figure 2 shows the design of such a proposed LAS system.

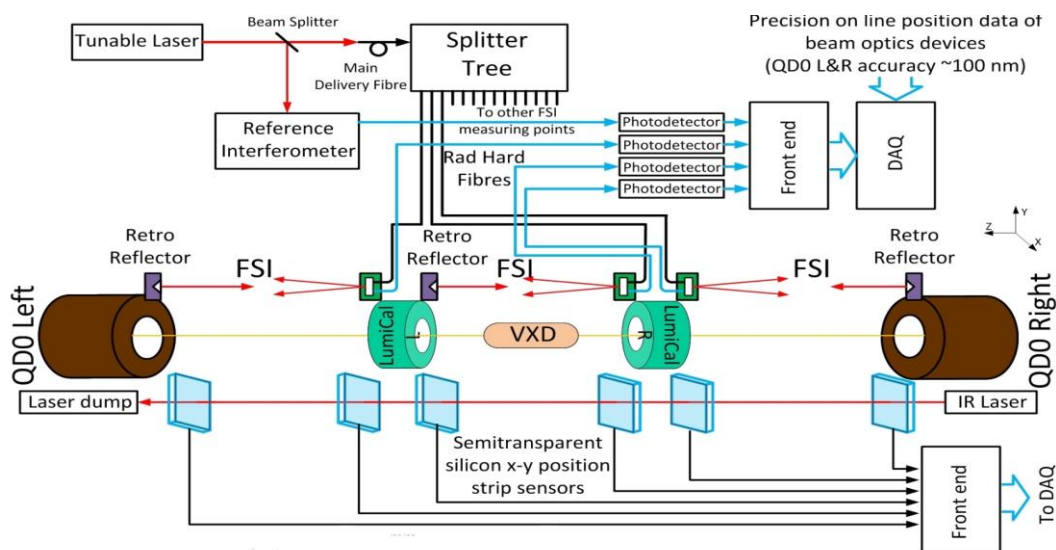


Figure 2. The design of the LAS system for LumiCal detector displacement.

This report will focus on the first component of the LAS system containing the semi-transparent silicon sensors (STS). To build a suitable prototype in the laboratory, the several components, which worked previously in the ZEUS experiment [11], were used. The prototype contains semi-transparent sensors (STS) with readout cards and diode lasers and were received from Oxford University. The semi-transparent amorphous silicon sensors, DPSD-516 [12], have light transmission above 85% for laser beam with > 780 nm within an active area of 5×5 mm², which allows several such sensors to be used in one laser beam. Each sensor contains 16 horizontal and 16 vertical strips (see Fig. 3) whose signals (after pedestal subtraction) are used to determine the mean position of the sensor in the X and Y directions.

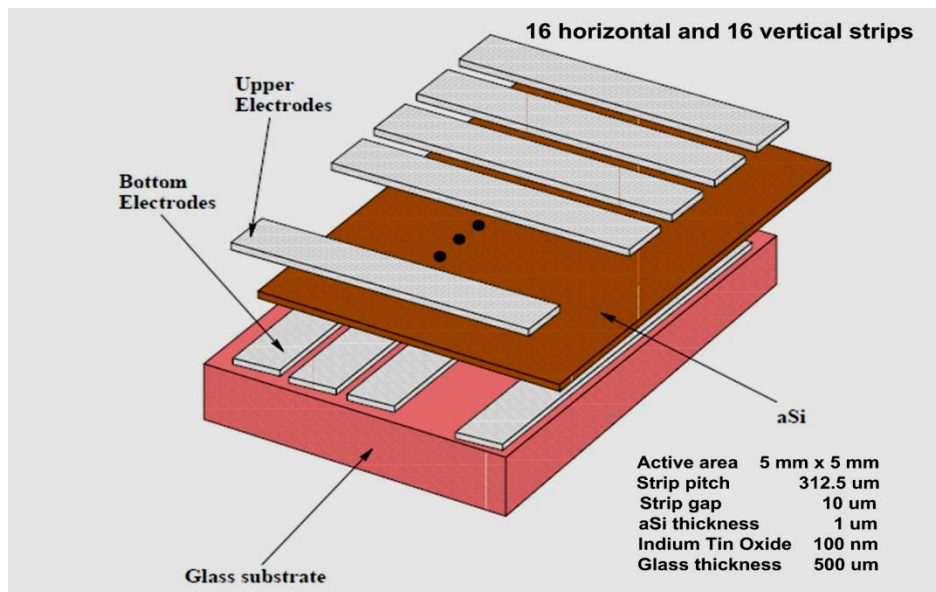


Figure 3. The schematic diagram of the DPSD-516 sensor.

The expected precision of such measurements is about 10 μ m. The STS sensors system can be applied to measure the LumiCal detector displacement over short distances, including the displacements of its internal sensor layers, or to determine the displacements of the LumiCal calorimeters relative to special reference frame like QD0 magnets. The semi-transparent sensors can be illuminated by lasers with power rating of about 5 mW. The special readout cables go from sensors to readout cards placed in the VME crate. The recovery of the VME system and re-installation of the LynxOS system allowed us to use a part of the old software associated with the collection of data from the strips.

3 Readout and software of position sensors

3.1 Hardware setup

A part of the alignment system for the ZEUS microvertex detector has been used [13] for reading sensors data. The hardware of the system is presented in Figure 4. It consists of the VME crate housing Motorola PowerPC VME Board running LynxOS 2.03 operating system, a ZEUS MVD 8 channels VME board for position sensors readout [14] and a VME module controlling the laser box [15], the laser box itself and a set of position sensors.

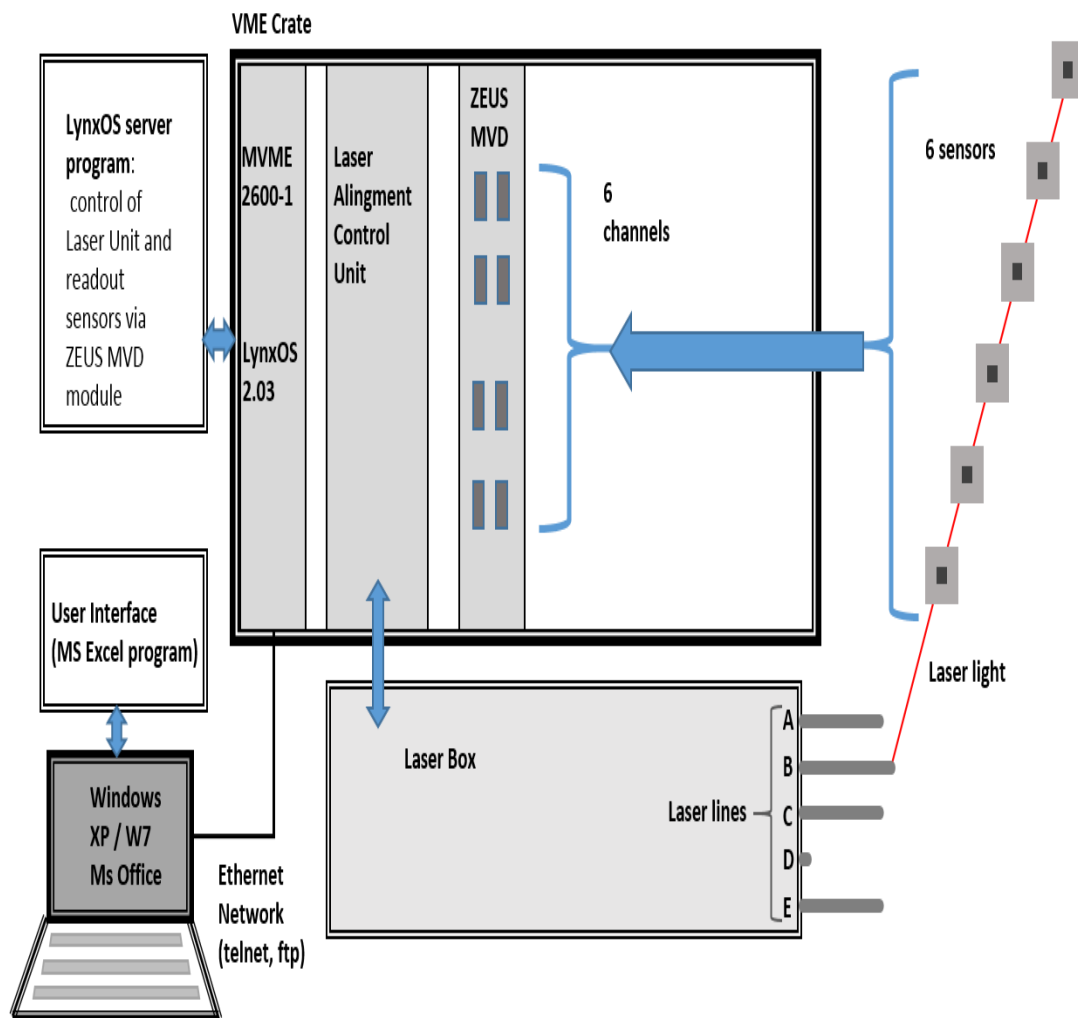


Figure 4. Hardware setup for position sensors readout.

3.2 Software

The software package for VMEbus access on Motorola PowerPC's running LynxOS, which has been created for the ZEUS MVD DAQ [16,17], has been used. A set of alignment control programs from the MVD alignment system was used for first tests and verification of the hardware and as a base for a simple server program. The test system (Figure 4) consists of the LynxOS station running a server program and a Windows PC running Microsoft Excel graphic user interface (GUI). The server works in a loop and waits for commands from a Windows computer. When a command arrives, sensors are readout in 2 steps: the first step is a pedestal (without laser signal) and in the second step the laser is set on. The data are stored in the local LynxOS directory in text files of a dedicated format and at the same time are sent to the Windows PC for display. The GUI program has been developed in Microsoft Excel, hence it can be launched in any Windows PC equipped with Microsoft Office. An example of the GUI window is presented in Figure 5.

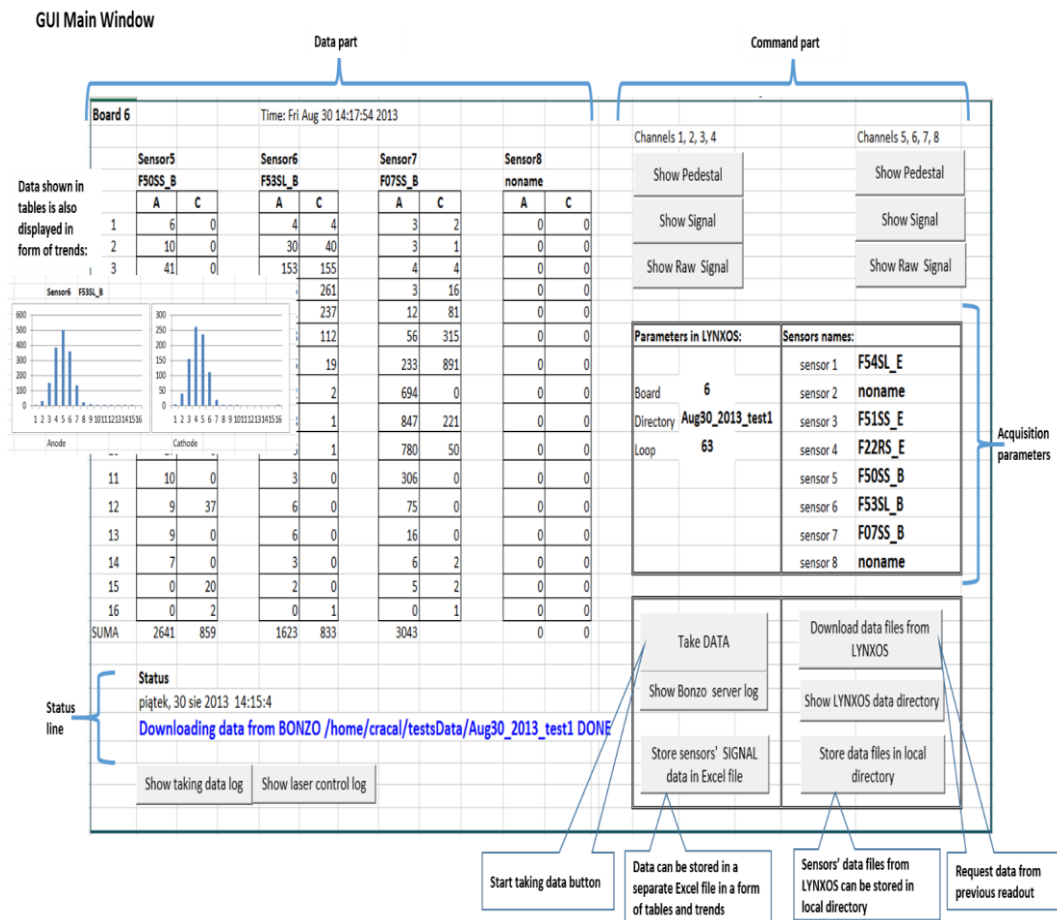


Figure 5. View of a User Interface.

The necessary parameters of the data acquisition, such as sensors' names, data file names and MVD properties, can be set. The data are displayed in a form of tables and trends. Moreover, there are some additional utilities: tables and trends can be stored in a separate Excel file for later use, LynxOS data files can be transferred to Windows PC and stored in a dedicated directory, also the data from previous readout sessions can be requested from LynxOS station and displayed. The connection between LynxOS station and Windows PC is based on telnet/ftp protocol.

4 Sensors

All received DPSD-516 sensors as well as all connecting cables were carefully tested . Each sensor contains 16 anode and 16 orthogonal cathode strips and with the strip pitch 312,5 microns, which forms an active sensor area of 5 x 5 mm². The thickness of amorphous silicon is about 1 micron. The detecting layer is deposited on ITO (indium tin oxide) cathode strips of 300 micron width, which are deposited on 500 microns thick supporting glass. The silicon layer, properly doped, is covered with 300 microns wide strips of transparent ITO behaving as rectifying anode contacts. The sensors structure and properties are described in detail elsewhere [11,12]. Figure 6 shows an encapsulated sensor bonded to specially developed cables.

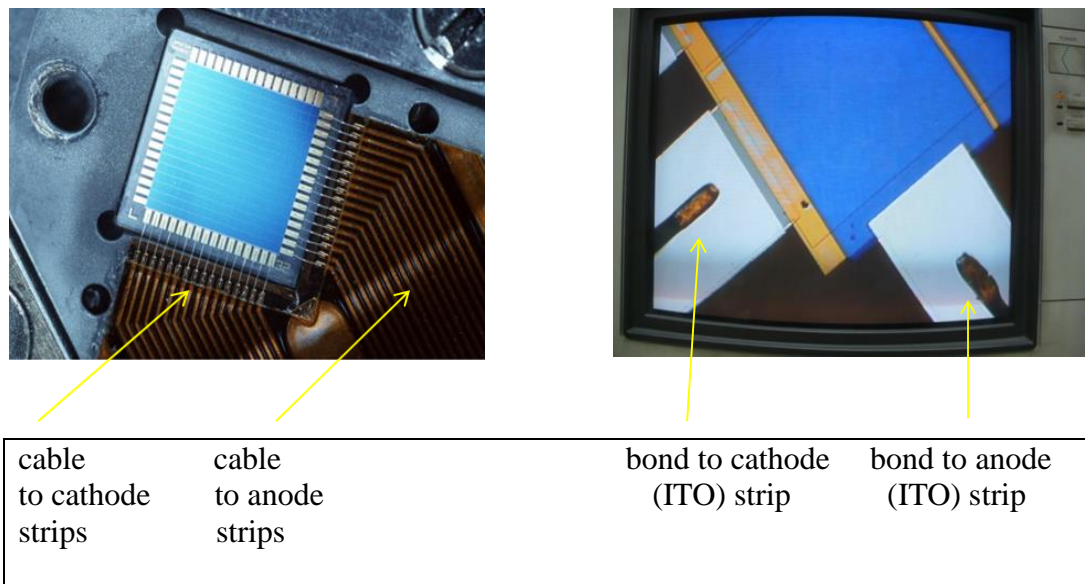


Figure 6. Photo of DPSD sensor with bonding of the flat cables.

Sixteen delivered sensors were tested for the presence of photoeffect in all strips. A special, simple holder was developed for these measurements. This holder allowed us also to check the capton cables used in the measurements. The daylight photoeffect of a few tens of mV was measured with a multimeter as the potential difference between strip and grounded strips of the opposite sensor side. Seven sensors which exhibit more than 30% of dead strips were rejected. Some of the strips selected for photoeffect have an enormously high current as could be seen in further measurements of ADC counts. It may be connected with a relatively strong electric field in silicon. At 3V applied to each sensor and 1 micron of thickness, there is a

field of 30 kV/cm which is a roughly critical value for avalanche breakdown in silicon. In the next step the sensors were tested on laser beam. A typical result is shown in Fig. 7 for sensor F53SL illuminated with laser beam.

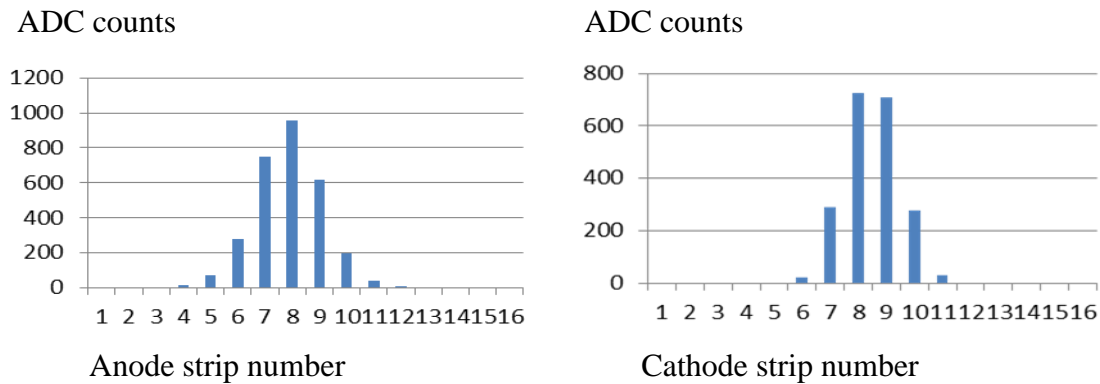


Figure 7. Results of measurement on sensor F53SL.

As can be seen, the values of ADC counts on the cathode strips are much smaller than on the anode strips. These differences are due to smaller mobility of the holes collected on the cathode in comparison with the mobility of electrons moving towards the anode. Despite a high value of the electric field in silicon, the holes' lifetime in this amorphous layer could be insufficient for full charge collection on the cathode. As a consequence, the cathode strips are more noisier than the anode ones and the cathode side of the sensor gives poorer line resolution.

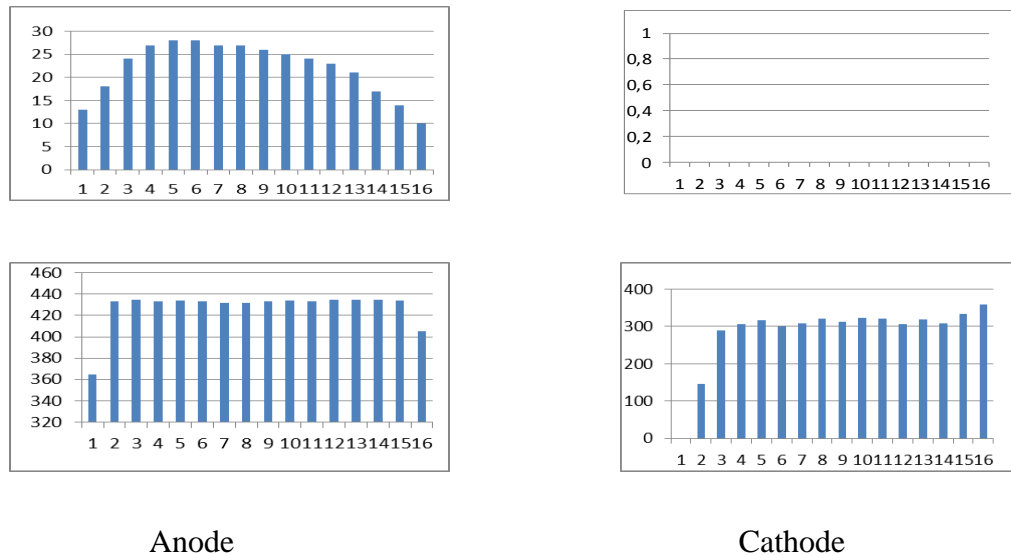


Figure 8. An example: The size of the individual strips signals upon irradiation of daylight.

To avoid scanning the sensor with the laser beam and to obtain information about the sensitivity of the boundary strips on the pulse of light, a simple method was used. It is illustrated in Fig. 8. The top diagrams show the measurements of the sensor illuminated with daylight from the anode side. Only weak signals on the anode are visible and no signals above channels thresholds on the cathode can be seen. Two bottom diagrams show results for

illumination with stronger light source: 100W electric lamp at 1 m distance from the sensor. In both measurements the pedestal was subtracted from a raw signal.

It is clear that direct illumination which does not necessarily come from the laser light allows the quality of the sensor to be easily determined and/or readout channels to be amplified. For example, the diagrams presented in Fig. 9 suggest which strips should be omitted in mean position calculations.

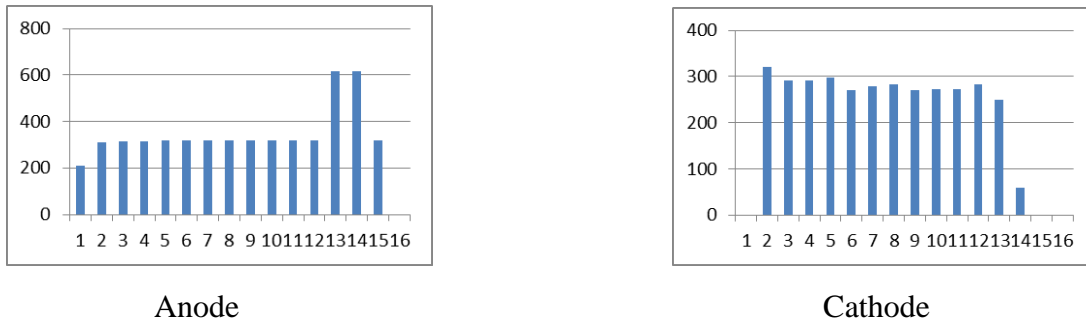


Figure 9. ADC counts for sensor F54SL illuminated with electric lamp.

In the next step, the selected good sensors were used to check readout channels in delivered electronics boards.

5 Data analysis and first results

Experimental setup consists of six sensors attached to optical table (Fig.10 left). Two of them (3-rd and 4-th – in plane3 and plane 4 respectively) are attached to the movable 3D stage. The beginning of coordinates is connected with the collimator of laser optical fiber, as schematically shown in Fig.10 left.

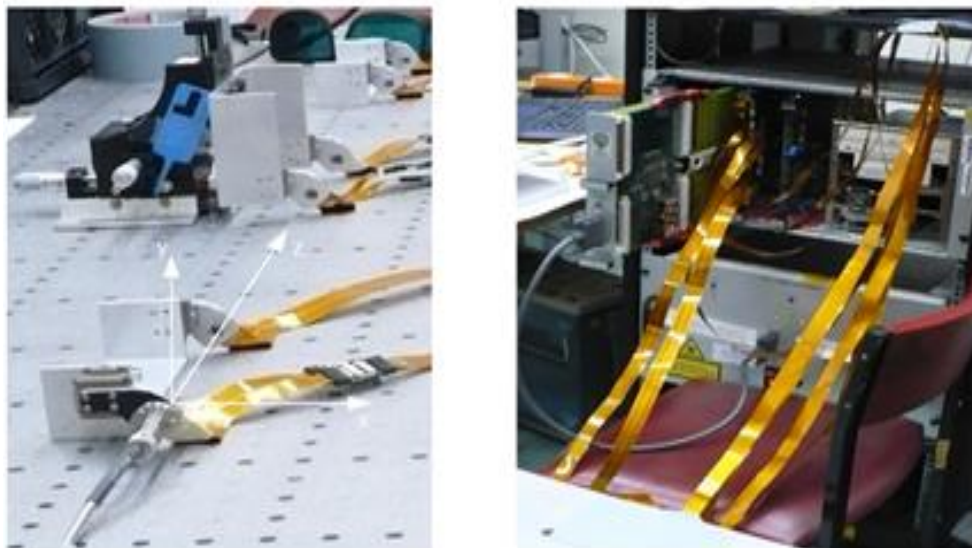


Figure 10. Left: Alignment system with sensor mounted on optical table. Right: Laser box and readout electronics for sensors used in the measurements.

The sensors define six XY planes with values of Z coordinate shown in Table 1. X-direction in each plane is perpendicular to anode strips of sensors.

Z1	Z2	Z3	Z4	Z5	Z6
2 cm	14 cm	50 cm	62 cm	92 cm	104 cm

Table1. Values of Z coordinate for sensor planes.

A relatively strong and low noisy laser beam was chosen for the measurements. Figure 11 and 12 show the beam-profile signals and Gaussian fits along one beam line. The attenuation of the laser intensity and beam broadening are evident as the number of sensors traversed increases. There is also evidence of smaller quantity of ADC counts for cathode (Y) side of sensors. The first attempt at analysis was to compare the mean sensor positions of laser beam relative to a reference run (usually the run with the lowest X value) of the period under study. The reason for plotting positions relative to a reference run is to allow the data from different runs to be plotted using a common scale. Figure 13 compares the mean position fluctuations for X (anode) and Y (cathode) directions for six planes and ten runs.

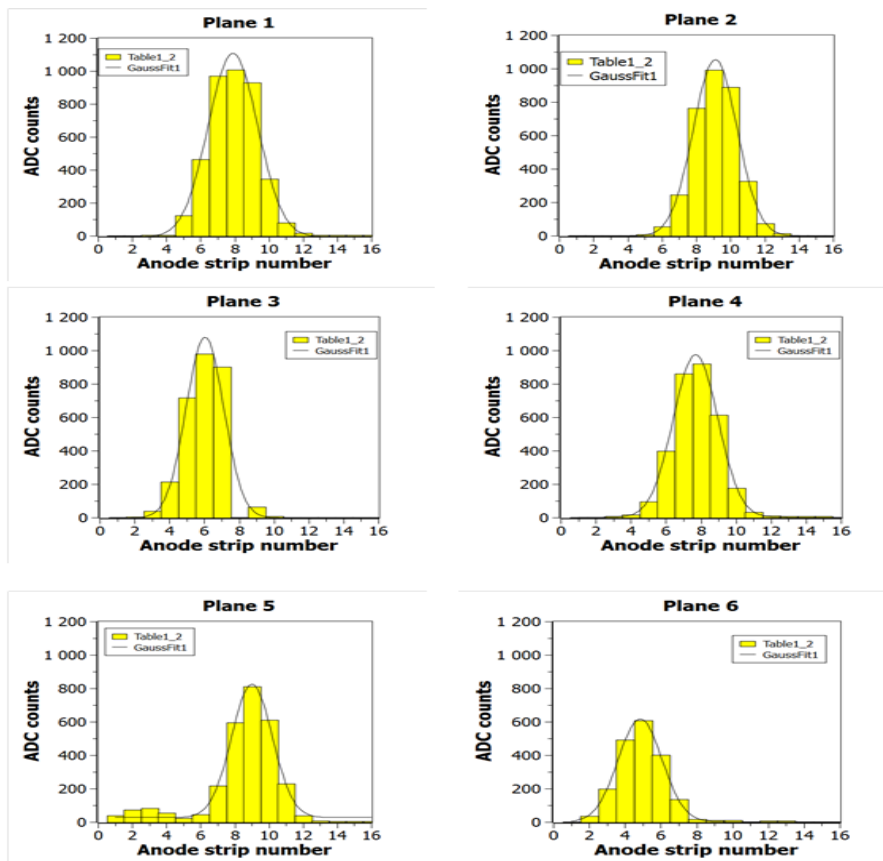


Figure 11. Examples of the beam-profile signals from the X-strips of sensors along beam line together with the Gaussian fits. The strip currents are in units of ADC counts and are plotted as functions of strip number.

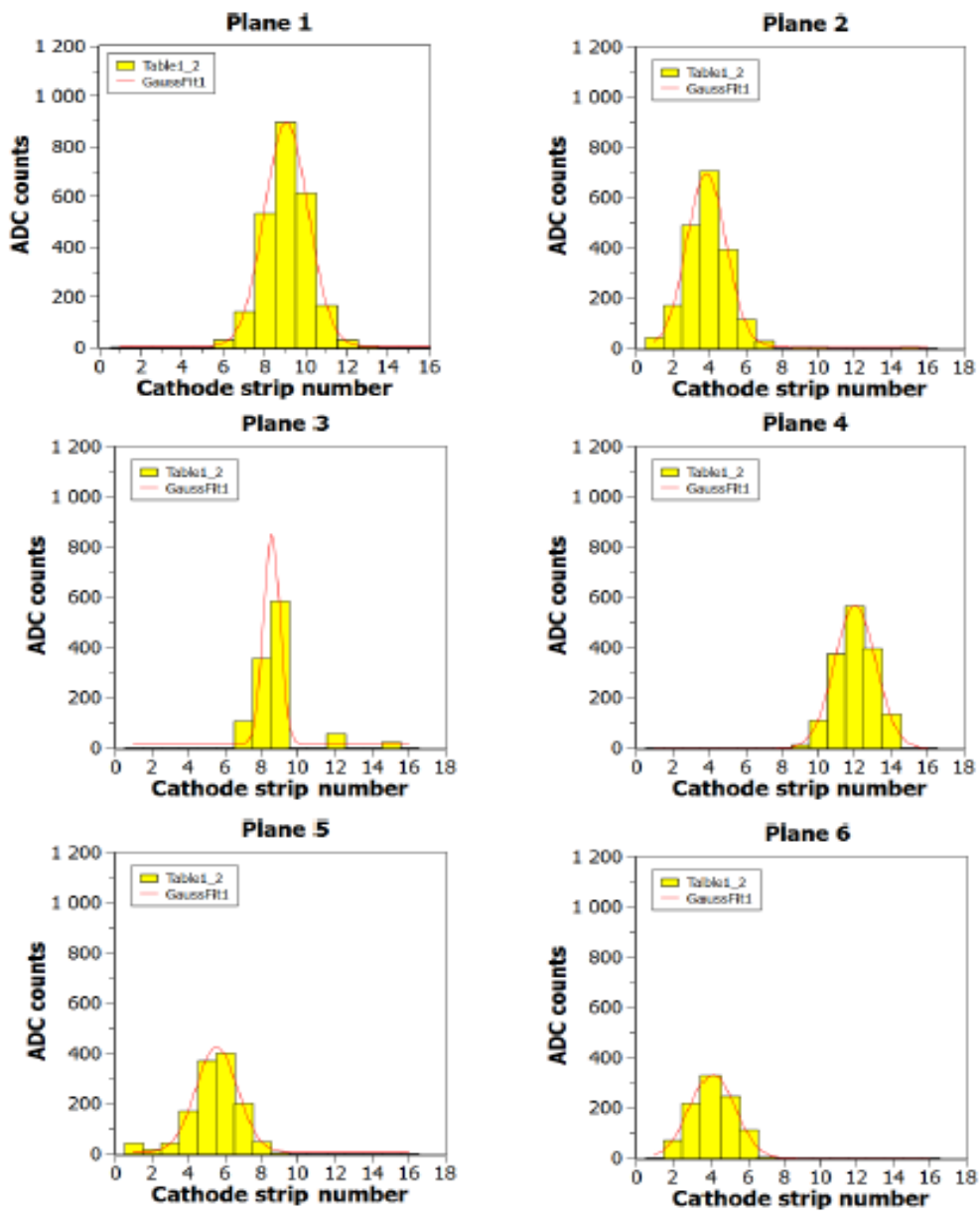


Figure 12. Examples of the beam-profile signals from the Y-strips of sensors along beam line, together with the Gaussian fits. The sensor in plane 3 probably lost contact (on cables or plugs) with strips 10, 11 and 13.

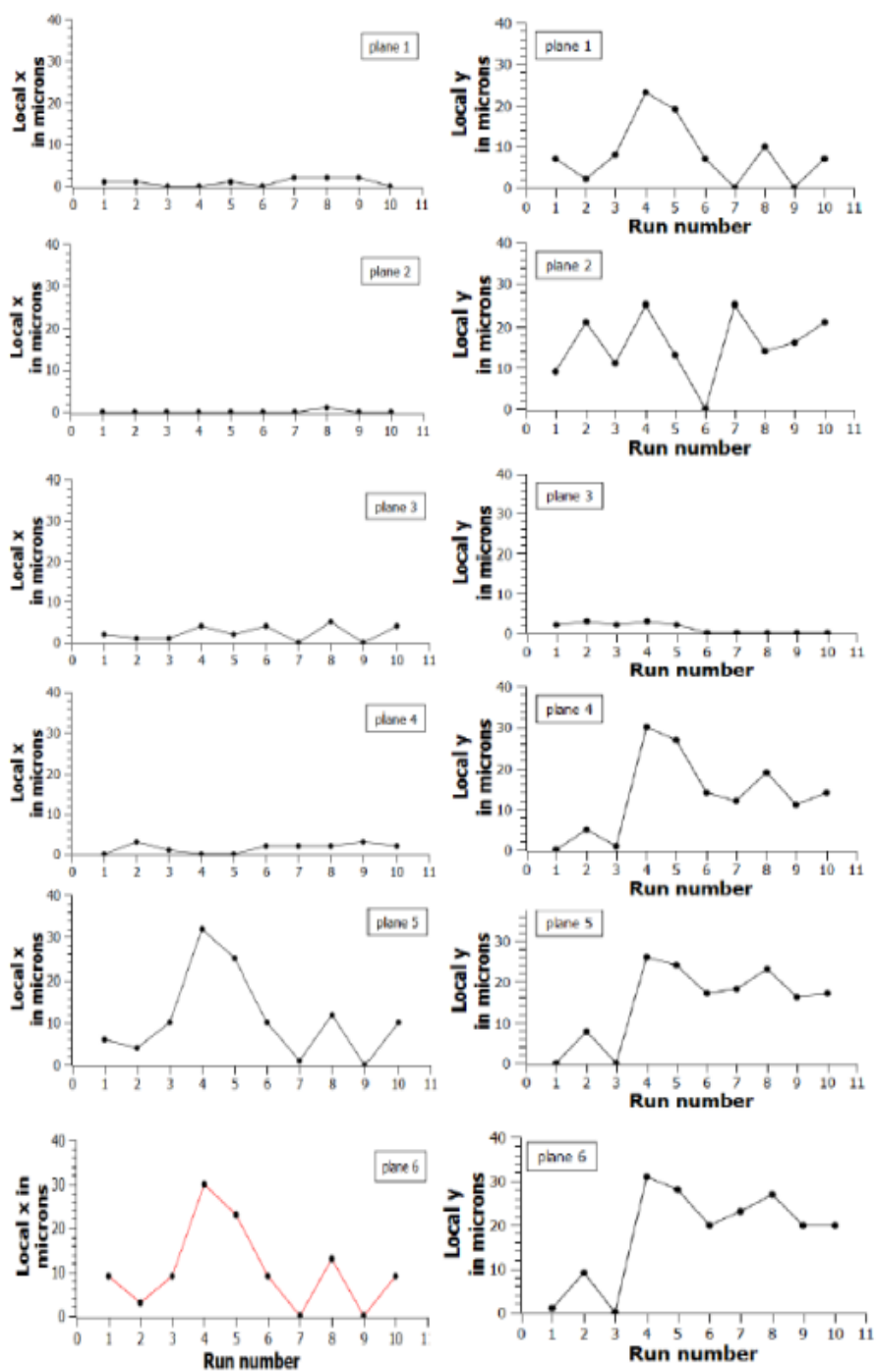


Figure 13. Relative positions of laser beam, in local coordinates, at the six planes starting with plane 1 at the top. The X (anode) and Y(cathode) signals are shown as functions of the run number (on left and right respectively). Small values of Y in plane 3 are connected with a few “dead” cathode strips.

Another example of the data for ten runs is shown in in Fig. 14. On the left hand one can see the results for six planes and ten runs performed with the laser “switched OFF” between the

period of data collecting. On the right hand, respectively, the laser was “switched ON” two hours before the first run and has been working continuously during measurements.

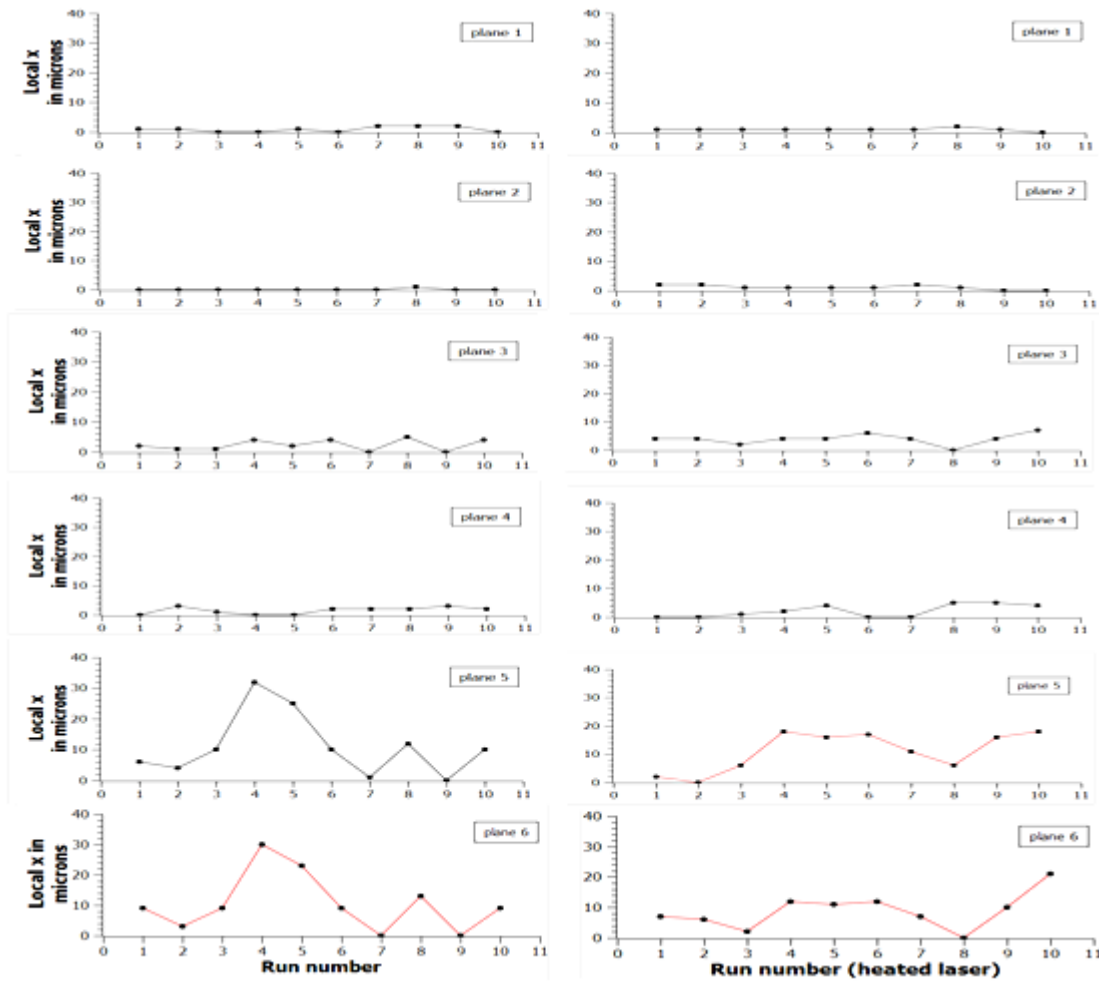


Figure 14. The relative positions of laser beam in local coordinates at six planes starting with plane 1 at the top. The X (anode) signals are shown as functions of the run number. Plots on the right side show runs with continuous laser work. The laser was heated 2 hours before runs.

The results of the measurements lead to the following remarks:

- the size of deviations tends to increase with distance along the laser beam;
- they are relatively large for cathode (Y) strips;
- there are some quite large deviations in planes 5, 6, up to 30 microns;
- a clear correlations between the larger deviations in different planes can be found;
- there is evidence that “heated” laser gives more reproducible results for different runs.

The difficult question to answer from this type of plots is whether this is evidence for movement of support or simply instabilities of the lasers and noise in the sensors. That is why an alternative procedure was developed for the analysis of the laser beam position data [11]. The idea is to define each beam line as an independent ‘straightness monitor’ which is illustrated schematically in Fig. 15.

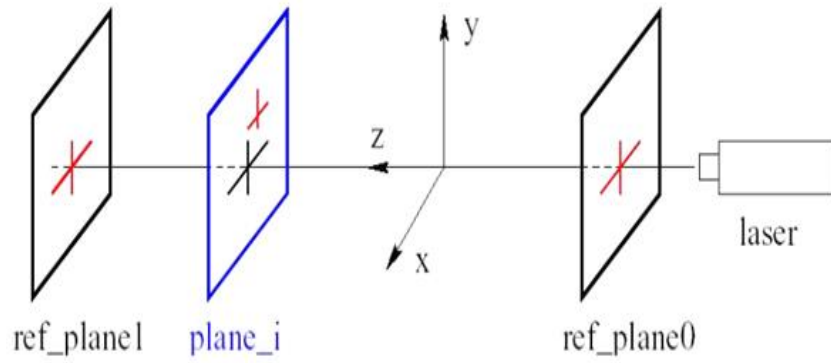


Figure 15. The procedure used to define the reference line for a given laser beam using the planes 1 and 0 (6 in our setup) and residual (offset) between the expected position and measured mean position in an interior sensor plane.

For a given laser beam and local coordinate the mean positions in sensor planes 1 and 6 are used to define the reference straight line. The expected relative position of the beam at a sensor plane, “i”, is then given in local sensor coordinates by:

$$\Delta x_i = \Delta x_1 \frac{z_6 - z_i}{z_6 - z_1} + \Delta x_6 \frac{z_i - z_1}{z_6 - z_1}$$

$$\Delta y_i = \Delta y_1 \frac{z_6 - z_i}{z_6 - z_1} + \Delta y_6 \frac{z_i - z_1}{z_6 - z_1}$$

The residuals in the two coordinate directions are calculated as the differences between the expected positions and the corresponding measured mean positions. Figure 16 shows the same data as displayed in Fig. 14 but the residuals are plotted relative to the line defined by planes 1 and 6 (hence the absence of deviations at these positions). Comparing Figures 14 and 16 one can see that the fluctuations are smaller, particularly in the planes furthest from the optical fiber laser head. There is evidence for movement or for further instabilities of the laser.

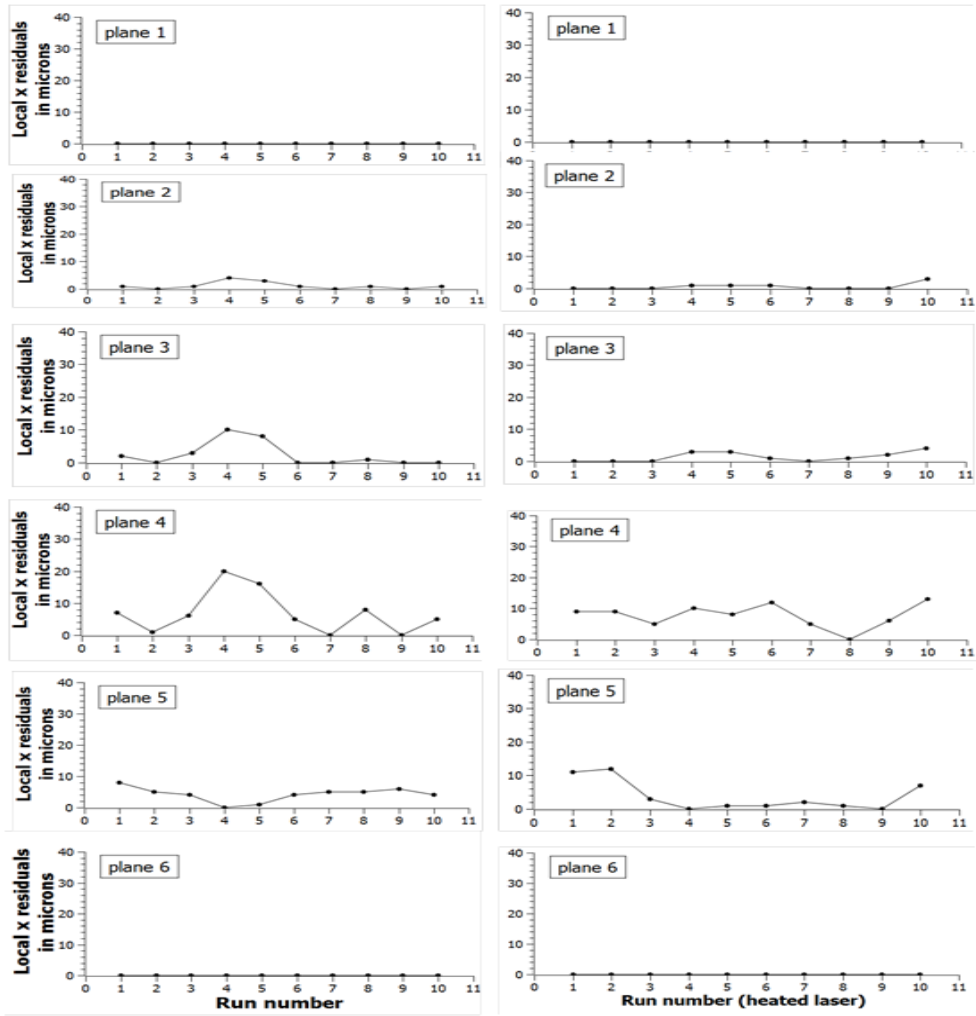


Figure 16. Residuals of laser beam in the local X coordinates.

Finally a movable stage was used to determine laser beam profile in plane 4. Dots are measured points (100 microns steps in X direction) and are fitted with a Gaussian. Results are presented in Fig. 17.

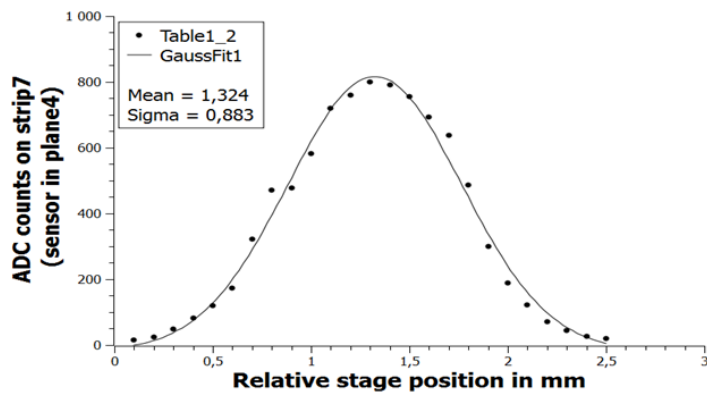


Figure 17. Shape of laser beam as measured on strip 7 of sensor in plane 4.

Conclusions

The prototype of the laser alignment system, LAS, containing the semi-transparent silicon sensors, STS, was built in the laboratory as one of the two elements of the proposed target system for monitoring movements of the luminosity detector LumiCal.

The preliminary measurements show the accuracy of laser beam mean position for sensor in plane 1 to be within ± 1 micron up to ± 16 microns in plane 6 for the anode side (X). For the cathode side (Y) such a value is ± 16 microns in all six planes. Since the mechanical displacement of sensors positions is practically excluded, the only source of bad position resolution in further planes seems to be inherent instabilities in laser beam. These instabilities may be also connected with the light passing through several layers of 500 microns thick supporting glass with unknown uniformity of thickness and surface reflection coefficient. The positive role of laser “heating” is evident.

The results of measurements of the STS sensors used previously in the ZEUS experiment confirm the possibility of using this type of sensors in target alignment system that has been proposed for the detector luminosity LumiCal. They would provide measurements of the relative X-Y displacement of the detector and its inner silicon sensors layers. It remains an open question whether this type of sensors will be available in the open market.

Acknowledgements

This work is partly supported by:

Commission under the FP7 Research Infrastructures project AIDA, grant agreement No. 262025.

The Polish Ministry of Science and Higher Education under agreement No. 2369/7.PR/2012/2.

We would like to thank R. Walczak for his great kindness and help in getting opportunities to use the optical elements of the laser alignment system built for ZEUS Micro Vertex Detector by University of Oxford and A. Polini for his invaluable and great help in restoring the operating system used during the sensors measurements.

References

- [1] **International Linear Collider Technical Design Report**, A. Abada et al., <http://www.linearcollider.org>.
- [2] **CLIC Conceptual Design Report**, A. Ioannisian et al., http://project-clic-cdr.web.cern.ch/project-clic-cdr/CDR_Volume1.pdf, CERN-2012-2007.
- [3] **Linear Collider Collaboration**: <http://www.linearcollider.org>.
- [4] International Large Detector (ILD), <http://ilcild.org>.
- [5] Silicon Detector (SiD), <https://confluence.slac.stanford.edu/display/SiD/home>.
- [6] FCAL Collaboration, <http://fcal.desy.de>.

- [7] H. Abramowicz et al., Forward Instrumentation for ILC Detectors, JINST **5** (2010) P12002.
- [8] Advanced European Infrastructures for Detectors at Accelerators (AIDA), <http://aida.web.cern.ch/aida/index.html>.
- [9] W. Daniluk et al., Laser Alignment System for LumiCal, EUDET-Report-2008-05; J. Aguilar et al., Laser Alignment System for LumiCal, EUDET-Memo-2010-08.
- [10] Hai-Jun Yang, Sven Nyberg and Keith Riles, High Precision absolute distance measurement using dual-laser frequency scanned interferometry under realistic conditions, Nucl. Instr. and Meth. A **575** (2007) 395;
Hai-Jun Yang et al., Frequency Scanned Interferometry for ILC Tracker Alignment, arXiv:1109.2582v1 [physics.ins-det], 2011.
- [11] K. Korcsak-Gorzo et al., The optical alignment system of the ZEUS microvertex detector, Nucl. Instr. and Meth. A **580** (2007) 1227;
K. Korcsak-Gorzo et al., The Optical Alignment System of the ZEUS Micro Vertex Detector, arXiv:0808.0836v1 [physics.ins-det], 2008.
- [12] W. Blum et al., A novel laser alignment system for tracking detectors using transparent silicon strip sensors, Nucl. Instr. and Meth. A **367** (1995) 413;
T. Matsushita et al., Optical alignment system for the ZEUS micro vertex detector, Nucl. Instr. and Meth. A **466** (2001) 383.
- [13] J. Ferrando, Ch. Youngman, The MVD Laser Alignment System Guide, ZEUS Note-05-013, 2005;
A. Polini et al., The design and performance of the ZEUS Micro Vertex Detector, Nucl. Instr. and Meth. A **581** (2007) 656.
- [14] N. Bazin, ZEUS Microvertex Readout Electronics. User Manual, June 2000, University of Oxford, Department of Physics, Nuclear & Astrophysics Laboratory. Central Electronics Group.
- [15] A. Polini, Laser Control Module, private information.
- [16] A. Polini, UVMELib: an easy approach to the VMEbus for Motorola PPC boards with Universe bridge and Lynx-OS, ZEUS Note 99-071, 1999.
- [17] A. Polini, The Architecture of the ZEUS Micro Vertex Detector DAQ and Second Level Global Track Trigger, Presented at 2003 Conference for Computing in High Energy and Nuclear Physics CHEP03, 2003, arXiv:physics/0307006v1 [physics.ins-det], 2003.

